Quaternary International 440 (2017) 13–22

Contents lists available at ScienceDirect

Quaternary International

journal homepage: www.elsevier.com/locate/quaint

Observational study on the active layer freeze–thaw cycle in the upper reaches of the Heihe River of the north-eastern Qinghai-Tibet Plateau

Qingfeng Wang [a], Tingjun Zhang [b, *], Huijun Jin [a, **], Bin Cao [b], Xiaoqing Peng [b], Kang Wang [b], Lili Li [b], Hong Guo [b], Jia Liu [b], Lin Cao [b]

[a] State Key Laboratory of Frozen Soil Engineering, Cold and Arid Regions Environmental and Engineering Research Institute, CAS, 320 Donggang West Road, Lanzhou, Gansu Province, 730000, PR China
[b] Key Laboratory of Western China's Environmental Systems, Ministry of Education, College of Earth and Environmental Sciences, Lanzhou University, 222 Tianshui South Road, Lanzhou, Gansu Province, 730000, PR China

ARTICLE INFO

Article history:
Available online 7 September 2016

Keywords:
Alpine permafrost regions
Active layer
Seasonal freeze–thaw cycle
Local factors
Upper reaches of the Heihe River (URHHR)
Qilian Mountains

ABSTRACT

Observational data collection on permafrost and active layer freeze–thaw cycle is extremely limited in the upper reaches of the Heihe River (URHHR) in the Qilian Mountains of the north-eastern Qinghai-Tibet Plateau. It acts as a bottleneck, restricting the hydrological effects of the changes in the permafrost and active layer in the Heihe River Basin. Using soil temperature, moisture and air temperature data collected from the four active layer observation sites (AL1, AL3, AL4 and AL7) established in the alpine permafrost regions in the URHHR, from 2013 to 2014, the region's active layer freeze–thaw cycle and the soil hydrothermal dynamics were comparatively analysed. As the elevation increased from 3700 m a.s.l. to 4132 m a.s.l., the mean annual ground temperatures (MAGTs) of the active layer and the active layer thicknesses (ALTs) decreased, the onset date of soil freeze of the active layer occurred earlier and the soil freeze rate increased. However, the onset date of soil thaw and the thaw rate did not exhibit significant trends. Compared to the thaw process, the duration of the active layer freeze process was significantly shortened and its rate was significantly higher. The soil freeze from bottom to top did not occur earlier than that from top to bottom. Furthermore, as elevation increased, the proportion of the bottom-up freeze layer thickness increased. The soil moisture in the thaw layer continuously moved to the freeze front during the active layer's two-way freeze process, causing the thaw layer to be dewatered. The seasonal thaw process resulted in significant reduction of the soil water content in the thaw layer, accounting for the high ice content in the vicinity of the permafrost table. Controlled by elevation, the active layer's seasonal freeze–thaw cycle was also affected by local factors, such as vegetation, slope, water (marsh water and super-permafrost water), lithology and water (ice) content. This study provides quantitative data that identify, simulate and predict the hydrological effects of the changes in the permafrost and active layer of the Heihe River Basin.

© 2016 Elsevier Ltd and INQUA. All rights reserved.

1. Introduction

The permafrost and talik distributions and the seasonal freeze–thaw cycles of active layers have profound effects on the hydrogeological conditions of cold regions. They play a critical role in groundwater formation and transport processes, distribution patterns and the water cycle modes of cold regions, by affecting the hydraulic connection of surface water and groundwater (Cheng and Jin, 2013). Permafrost degradation caused by climate change has significantly changed the hydrogeological environment of cold regions (Serreze et al., 2000; Cao et al., 2003; Zhang et al., 2013), which will have significant effects on the hydrological processes in the source regions of rivers. Such effects include the decrease of the super-permafrost water table, the increase in vadose zone thickness, the reduction in storage capacity of the water resource and the degradation of the ecological environment (Wang et al., 2002;

* Corresponding author.
** Corresponding author.
E-mail addresses: tjzhang@lzu.edu.cn (T. Zhang), hjjin@lzb.ac.cn (H. Jin).

http://dx.doi.org/10.1016/j.quaint.2016.08.027
1040-6182/© 2016 Elsevier Ltd and INQUA. All rights reserved.

Cao et al., 2003; Zhao and Zhou, 2005), especially in discontinuous permafrost zones (ACIA, 2005; Hinzman et al., 2005). Therefore, the study of the hydrological effects of permafrost degradation in the source regions of rivers is of great significance for assessing changes in water resources in cold regions, and maintaining regional ecological security and sustainable development. However, observational data collection on permafrost and active layer freeze–thaw cycle is extremely limited in the upper reaches of the Heihe River (URHHR) in the Qilian Mountains of the north-eastern Qinghai-Tibet Plateau (QTP). It acts as a bottleneck, restricting the hydrological effects of the changes in the permafrost and active layer of the Heihe River Basin.

Active layer freeze–thaw cycles and the soil hydrothermal dynamics are affected by climate conditions, snow cover, vegetation, topography (elevation, aspect and slope), water (swamp water, lakes, river and super-permafrost water), lithology and water content (Zhou et al., 2000). Local and international studies have mainly focused on the tundra in northern Alaska, the Da Hinggan Mountains, the Three Rivers source regions, and the north-eastern QTP and other places along the Qinghai-Tibet Highway and Railway. The previous pertain to a tundra climate, a humid climate in the cold temperate zone, a humid climate north of a mid-temperate zone and a semi-arid climate and an arid climate in the alpine zone, respectively. Some preliminary conclusions regarding the effect of local factors on active layer freeze–thaw cycles have been made. The simulated results of a one-dimensional heat transfer model showed that variations in tundra snow density had a limited effect on the active layer thickness (ALT), but demonstrated a strong effect on the ground temperature of the Alaska North Slope (Ling and Zhang, 2006). Ground surface organic matter showed a buffering effect on soil temperature change in the tundra and boreal forest zones (Nicolsky et al., 2007). In the source region of the Yangtze River (Wang et al., 2008, 2012; Hu et al., 2009a, b; Wang et al., 2012) and the Yellow River (Luo et al., 2014) on the QTP, in the regions along the Qinghai-Tibet Highway (Li et al., 2012) and Railway (Wu et al., 2015) and in the northern Da Hinggan Mountains (Chang et al., 2015b), field observations showed that vegetation had an observable effect on the active layers' freeze–thaw cycles and soil hydrothermal dynamics. The hydrograph of the super-permafrost water was similar to the soil moisture dynamics pattern in the Fenghuoshan Mountains (Wang et al., 2009; Chang et al., 2015a). Based on the recharge relationships among ground ice, precipitation, and river water in the Beiluhe Basin on the central Qinghai-Tibet Railway, subsurface ground ice was partly recharged by precipitation and river water (Yang et al., 2013b). The distributions of different carbon components and stable carbon isotopes in the active layer and permafrost were analyzed in the peatland of the Eboling Mountains in the URHHR (Mu et al., 2014). However, there are only sporadic reports on the seasonal freeze–thaw cycle of the active layer in the URHHR in the Qilian Mountains.

Systematic research on the active layer seasonal freeze–thaw cycle and soil hydrothermal dynamics in the URHHR is required to determine the hydrological effects of the changes in the permafrost and active layer of the Heihe River Basin. Using soil temperatures, moistures and air temperatures measured at the four observation sites in the alpine permafrost regions of the URHHR in the north-eastern QTP (Fig. 1), the active layer's seasonal freeze–thaw cycle, soil hydrothermal dynamics and influencing factors were systematically analysed.

2. Study area

Located in the QTP's northern permafrost zone, the URHHR in the Qilian Mountains belongs to the Altun to Qilian Mountains alpine permafrost sub-zone (Zhou et al., 2000). The climate is subfrigid and semi-arid, and the alpine permafrost and seasonal frozen

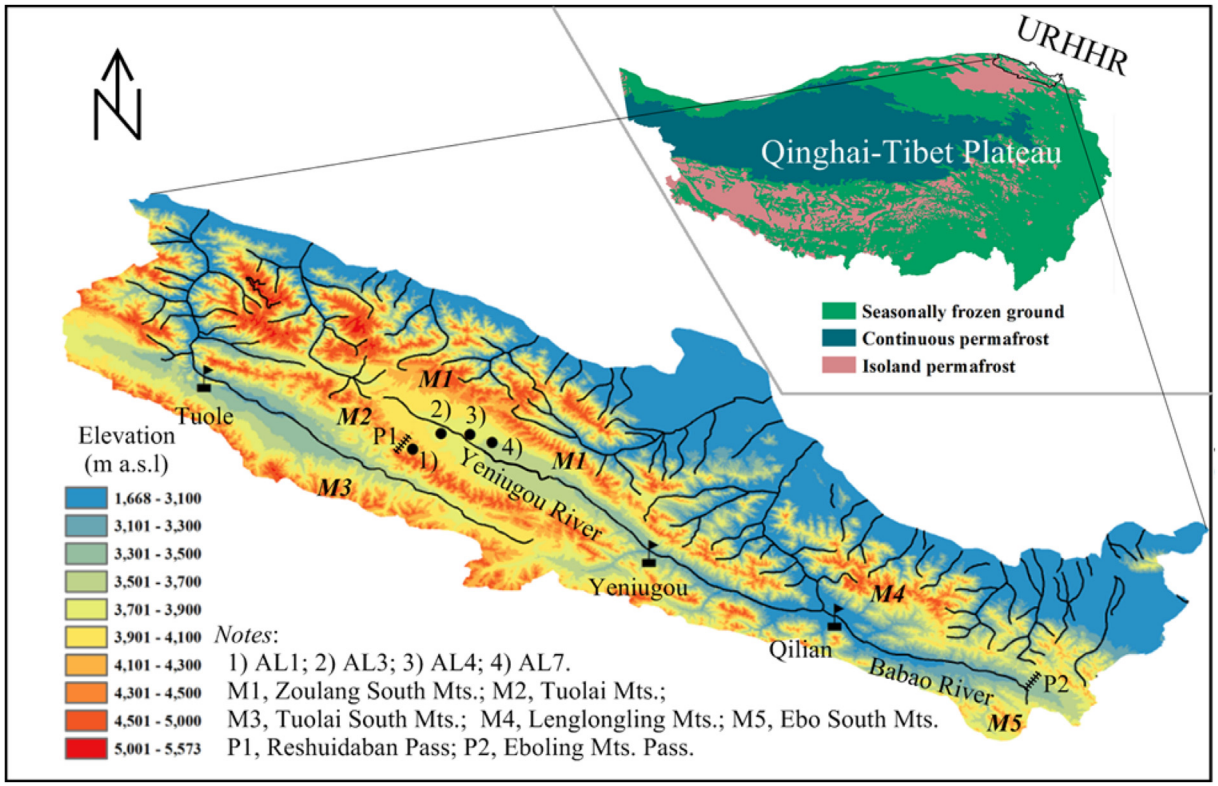

Fig. 1. The location of the URHHR, in the north-eastern QTP, and the active layer observation sites.

ground are well developed (Fig. 1). According to observational data from the China Meteorological Administration, the mean annual air temperatures (MAATs) in the Qilian, Yeniugou and Tuole stations, in 1957/1959–2004, were −3.0 °C, −2.9 °C and 0.7 °C, respectively, and the annual precipitation was 403 mm, 404 mm and 286 mm, respectively (Wang et al., 2013).

The vegetation in the URHHR is classified as temperate mountain forest steppe, with a patchy or blocky distribution of shrubs and trees. The altitudinal zonation of vegetation and soil is extremely evident. It is made up of an alpine shrub meadow zone, an alpine meadow zone and an alpine cushion vegetation zone from bottom to top. Similarly, the main types of soil are alpine shrub meadow soil, alpine meadow soil and cold desert soil. In the west branch (the Yeniugou River) of the URHHR, the lower boundary of alpine permafrost is 3650–3700 m a.s.l. There is no permafrost on the sunny slope of the Eboling Mountains in the east branch (the Babao River), and the lower boundaries of the alpine permafrost and isolated alpine permafrost on the shady (north) slope are 3600 m a.s.l. and 3390 m a.s.l., respectively (Fig. 1).

3. Experimental design and data acquisition

Four active layer observation sites (AL1, AL3, AL4 and AL7) were established between the Reshuidaban Pass and the low boundary of the alpine permafrost in the alluvial plain in the west branch of the URHHR in early October 2012, with elevations decreasing from 4132 m a.s.l. to 3700 m a.s.l. (Fig. 1). The aim was to investigate the differences in the active layer's seasonal freeze–thaw cycle and the effects on a cross-section from the pass to the plain in alpine permafrost regions. Differences in elevation, mean annual ground temperature (MAGT) and lithology were considered.

The AL1 site is located on the gentle slope in front of the Reshuidaban Pass, with widely developed hummocks and silty loam and loam lithology. The AL3 site is located on the piedmont sloping plain, with loam and sandy loam lithology. Located in the alluvial plain, the lithology of the AL4 site is sandy loam and sand, whereas that of the AL7 site is sand and sandy loam (Table 1). The vegetation types of the AL1, AL3, AL4 and AL7 sites are alpine swamp meadow, alpine meadow, alpine grassland and alpine grassland, respectively, with vegetation coverage of 94, 85, 85 and 80%, respectively. The dominant species at the AL1 and AL3 sites is the Tibetan Kobresia (*Kobresia tibetica Maximowicz*), whereas it is the Kobresia pygmaea (*Kobresia pygmaea C. B. Clarke*) at the AL4 and AL7 sites. The ALTs at the AL1, AL3, AL4 and AL7 sites are 1.6 m, 2.2 m, 3.6 m and 3.9 m, respectively, and the MAGTs are −1.9 °C, −1.4 °C, −0.3 °C and −0.1 °C, respectively (Table 1). According to the meteorological data from the AL1, AL3, AL4 and AL7 sites, and the Yeniugou and Qilian stations of the China Meteorological Administration, the study area's MAAT and annual precipitation are approximately −4.0 °C and 400 mm, respectively (Fig. 1). Therefore, the climate conditions are relatively similar in the study area.

According to the active layer lithology and practical conditions, soil temperature and soil moisture probes were installed at the four sites as shown in Fig. 2. Soil temperature and water content were measured using the 109 Temperature Probe and the CS616 Water Content Reflectometer from Campbell Scientific, Inc. The measurement range of the 109 Temperature Probe is −50–70 °C, and its maximum linearization error is 0.03 °C at −50 °C. With the resolution of <0.1%, the CS616 Probe accuracy is ±2.5% using standard calibration with a bulk electrical conductivity of ≤0.5 dS m^{-1} and a bulk density of <1.55 g cm^{-3} for a volume water content (VWC) measurement range of 0–50%. It is important to note that only the VWC of the liquid water could be measured by the CS616 probe, thus only the VWC of the unfrozen water was measured during the cold seasons. The probes were powered by solar panels through a battery, and the CR1000 data logger produced by Campbell Scientific, Inc. was used for data acquisition. Air temperature was measured using the HOBO Pro V2 (U23) produced by the Onset Computer Corporation, which was placed in the thermometer shelter that had been installed in advance. Its measurement range is −40–70 °C, with an accuracy of ±0.2 °C and a resolution of 0.02 °C. Air temperature measurement at the AL1, AL3 and AL4 sites began in March 2012, whereas air temperature measurement at the AL7 site began in October 2012. The observation interval for all of the above instruments was 30 min.

The soil temperature and moisture data used in this paper are from 1 January 2013 to 30 November 2014. The air temperature data are from 1 January 2013 to 31 December 2013. We focus on the active layer's freeze–thaw cycle and soil hydrothermal dynamics from the onset date of the soil thaw process in 2013 through to that in 2014.

4. The active layer freeze–thaw cycle and variations in soil hydrothermal dynamics

The active layer freeze–thaw cycle can be divided into three stages: the seasonal thaw process, the seasonal freeze process and the completely frozen stage in which the soil temperature of the whole active layer is negative (Hinkel and Nicholas, 1995; Osterkamp and Romanovsky, 1997; Romanovsky and Osterkamp, 1997; Zhao et al., 2000; Wang et al., 2012).

4.1. The seasonal thaw process

The AL1, AL3, AL4 and AL7 sites began to thaw stably from top to bottom in early or mid-April, and stopped in early October. The thaw depth at the AL1 site was 7 cm on 18 April and 27 cm on 7 May. It began to decrease from 8 to 20 May and then continued to thaw downwards. The thaw depth at the AL1 site reached a maximum in mid-September and was maintained until early October (Fig. 3A). This was a result of the large amount of ice contained in the soil near the permafrost table that needed to absorb a large amount of latent heat during the ice phase transition. The duration of the seasonal thaw process was

Table 1
Summary of the active layer observation sites in the alpine permafrost region in the URHHR

Sites	Elev (m)	MAAT (°C)	GSTAR (°C)	ALT (m)	MAGT (°C)	PT (m)	Vegetation type	Lithology
AL1	4132	−4.3	28.1	1.6	−1.9	111	ASM	Silty loam, loam
AL3	3843	−3.9	28.7	2.2	−1.4	107	AM	Loam, sandy loam
AL4	3775	−4.4	28.9	3.6	−0.3	23.5	AG	Sandy loam, sand
AL7	3700	−4.1	28.4	3.9	−0.1	13	AG	Sand, sandy loam

Note: MAAT = mean annual air temperature; GSTAR = ground surface temperature annual range; PT = permafrost thickness; ASM = alpine swamp meadow; AM = alpine meadow; AG = alpine grassland.

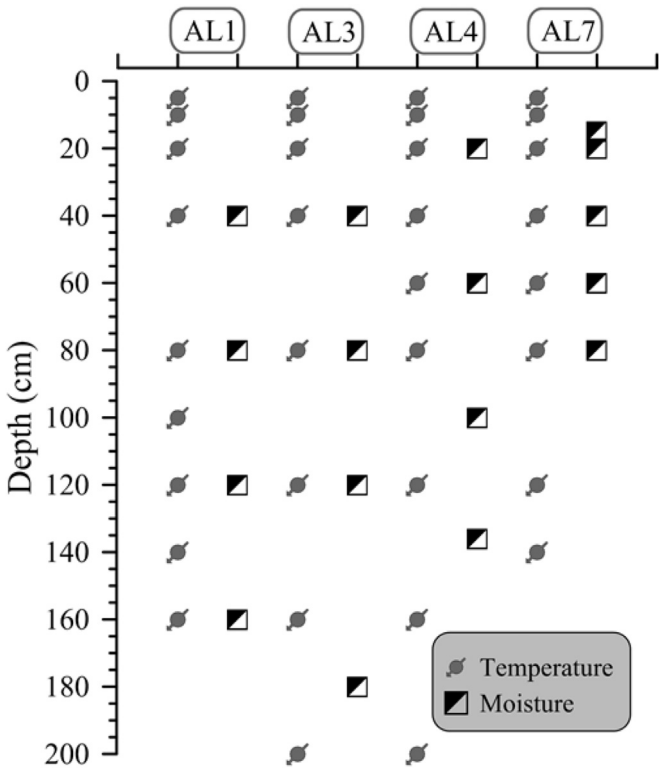

Fig. 2. The installation depth of the soil temperature and moisture probes at the active layer observation sites.

approximately 139 d, and the average thaw rate was 1.1 cm d^{-1}. The thaw depths at the AL3, AL4 and AL7 sites were 5.5 cm, 7 cm and 7 cm on 24, 16 and 22 April, respectively. They increased to 200 cm, 200 cm and 140 cm on 18 August, 21 July and 9 July, respectively (Fig. 3B–D).

As air temperatures rise, the active layer is heated by the atmosphere, resulting in a seasonal thaw process that occurs from top to bottom. The direction of soil heat flux is downwards, thus, the soil is in an endothermic state. Soil moisture migration is mainly from top to bottom throughout the process, which entails free water migration from top to bottom, caused by gravity, in the active layer above the thaw front; capillary water migration from bottom to top, water vapour evapotranspiration and convection due to the evaporation of surface water (Hinkel and Nicholas, 1995); and the migration of unfrozen water from top to bottom in the frozen soil (Cheng, 1982; Zhao et al., 2000). The soil temperature distribution pattern of the active layer formed at the end of the seasonal thaw process is the top higher and the bottom lower, whereas the distribution pattern of soil moisture is the bottom and central higher and the top lower (Figs. 3–5). For example, soil temperatures at a depth of 5 cm were higher than the values at the bottom of the AL1, AL3, AL4 and AL7 sites by 1.1 °C, 2.2 °C, 2.2 °C and 0.5 °C, respectively, in early October 2013 (Fig. 5). The high value of near-surface soil moisture formation is due to occasional short-term precipitation events (Fig. 4A and C). Affected by 'thaw steps' in the phase change of ground ice during the process of the thaw front gradually moving downwards (Zhou et al., 2000), unfrozen water content contour lines also exhibit a stepped shape and the unfrozen water content is higher closer to the thaw front (Fig. 4). Conductive and non-conductive heat transfer is active above the thaw front, whereas conductive heat transfer is dominant below the thaw front (Zhao et al., 2000).

4.2. The seasonal freeze process

Unlike the freeze process of the seasonal freezing layer in the seasonally frozen ground regions, the two-way seasonal freeze process (i.e., from top to bottom and from bottom to top) is observed in the active layer. In general, as latitude and elevation increase, the proportion of the freeze layer thickness from bottom to top increases (Zhou et al., 2000).

The AL1 site began the two-way seasonal freeze process in early October. The freeze front from top to bottom was at depths of 8 cm, 23 cm and 91 cm on 10, 19 and 23 October, respectively. The freeze front from bottom to top was at depths of 160 cm, 150 cm and 105 cm on 14, 19 and 23 October, respectively. The two freeze fronts met at a depth of 100 cm on 24 October, ending the seasonal freeze process (Fig. 3A). For the soil at depths of 5–160 cm, the freeze thickness and rate from top to bottom (92 cm and 6.1 cm d^{-1}) were significantly greater than the freeze thickness and rate from bottom to top (60 cm and 5.5 cm d^{-1}). Thus, the freeze thicknesses from top to bottom and from bottom to top were 62.5% and 37.5% of the maximum seasonal thaw depth, respectively.

The AL3, AL4 and AL7 sites began to freeze from top to bottom in mid- or late October. The freeze depth at the AL3 site from top to bottom was at 8 cm, 117 cm and 198 cm on 16 October, 4 November and 14 November, respectively. It was estimated that the two freeze fronts merged into one, reaching a depth of 200 cm on 16 November (Fig. 3B). Considering the ALT of 2.2 m, the freeze thicknesses from top to bottom and from bottom to top were 91% and 9% of the maximum seasonal thaw depth, respectively. The freeze depth from top to bottom at the AL4 site was at 5 cm, 80 cm and 200 cm on 20 October, 21 November and 3 December, respectively (Fig. 3C). The freeze depth from top to bottom at the AL7 site was at 11 cm, 97 cm and 140 cm on 24 October, 2 December and 7 December, respectively (Fig. 3D).

It is concluded that, in general, if the MAGT is approximately or ≤ -2 °C, the onset date of soil freeze from bottom to top will occur earlier than that from top to bottom. However, with a MAGT > -2 °C, and if there is super-permafrost water, a high soil water content at the bottom of the active layer or an absence of snow, the onset date of soil freeze from bottom to top will occur later than or simultaneously to the soil freeze from the top to bottom (Zhou et al., 2000). The MAGT at the AL1 site was approximately -2 °C (Table 1), but on account of a soil water content as high as 0.44–0.46 at the bottom of the active layer (Fig. 4A), the onset date of soil freeze from bottom to top occurred at least 4 d later than that from top to bottom. With MAGTs at the AL3, AL4 and AL7 sites all significantly higher than -2 °C (Table 1), the onset date of soil freeze from bottom to top did not occur earlier than that from top to bottom. Thus, the duration of soil freeze at the AL1 and AL3 sites was 15 d and 32 d, respectively, even shorter than the duration of soil thaw. It can also be concluded that, as elevation decreases, the soil freeze thickness from bottom to top at the AL4 and AL7 sites occupied significantly <9% of the maximum seasonal thaw depth.

During the freeze process, the active layer almost becomes a closed system in the study area. The soil temperature is high in the central part of the active layer and low in the upper and lower active layer. It is 0 °C or slightly above 0 °C in the thaw layer between the two freeze fronts (Fig. 3). The conductive heat transfer is almost zero, and the thermal exchange coupled with water vapour distillation and convection, driven by an osmotic gradient, is the main method of heat transport (Outcalt et al., 1990; Outcalt and Hinkel, 1992). The moisture in the thaw layer continuously moves to the freeze front, causing the thaw layer to be dewatered and the heat to be released due to the

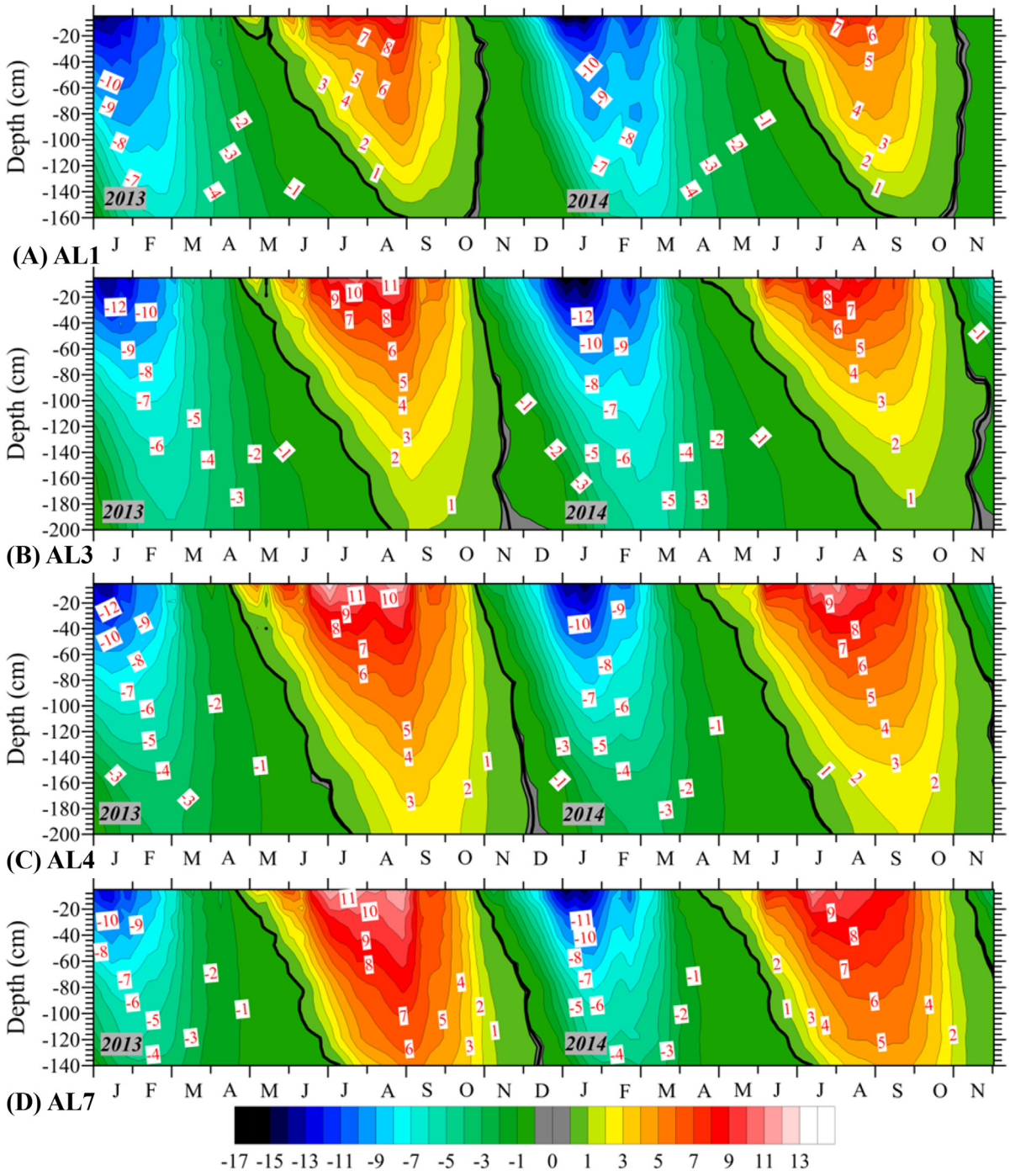

Note: The bold gray line represents the 0 °C isotherm. The gray area represents the error range of the 0 °C isotherm (± 0.03 °C).

Fig. 3. The soil temperature dynamics in the active layer of the URHHR.

phase change moving to the areas above and below the freeze front (Zhao et al., 2000). For example, during the seasonal freeze process from 10 to 23 October, soil moistures at depths of 40 cm, 80 cm and 120 cm at the AL1 site decreased by values of 0.015, 0.023 and 0.024, respectively (Fig. 6). However, soil moisture migration is always in the way of unfrozen water migration in the freeze layer, which causes soil hydrothermal coupling migration.

4.3. The completely frozen stage

From when the whole active layer freezes through to the onset of stable thawing at the ground surface the following year, the soil temperature of the whole active layer is negative. This is called the 'completely frozen stage'. The duration of the completely frozen stage at the AL1, AL3, AL4 and AL7 sites was 193 d, approximately 145 d, <131 d and <124 d, respectively.

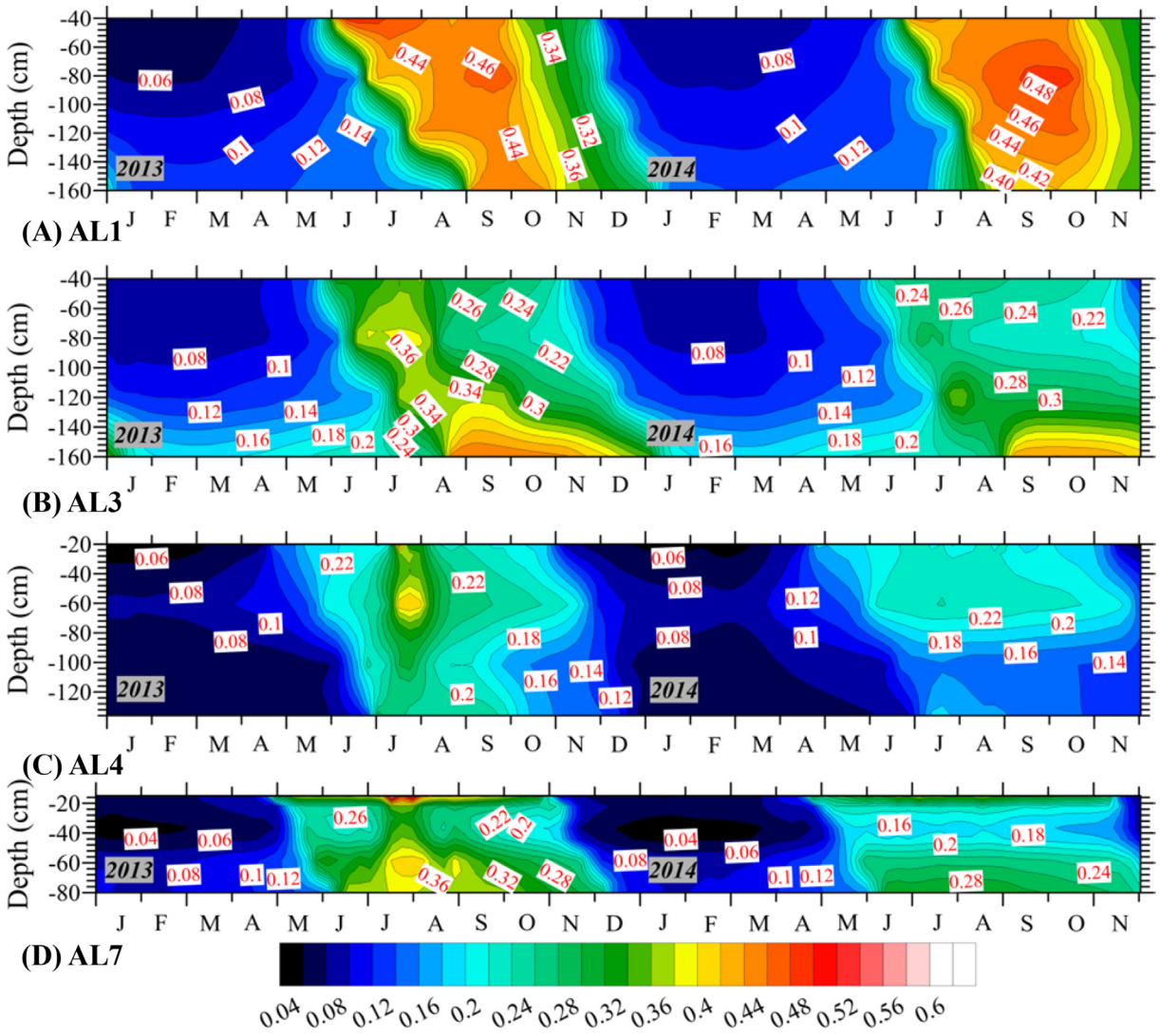

Fig. 4. The soil moisture dynamics in the active layer of the URHHR.

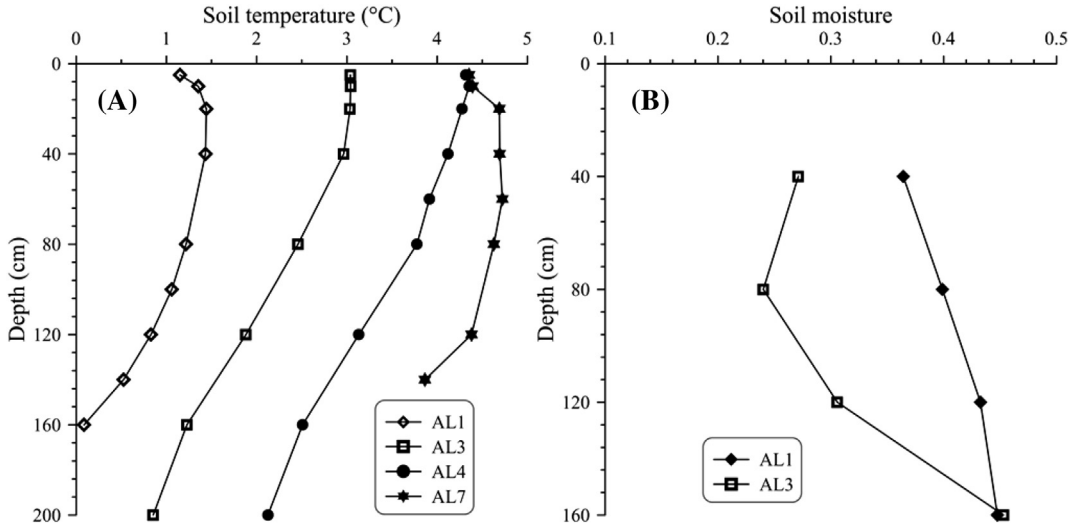

Fig. 5. The (A) soil temperature and (B) moisture distributions of the active layer at the end of the seasonal thaw process in early October 2013.

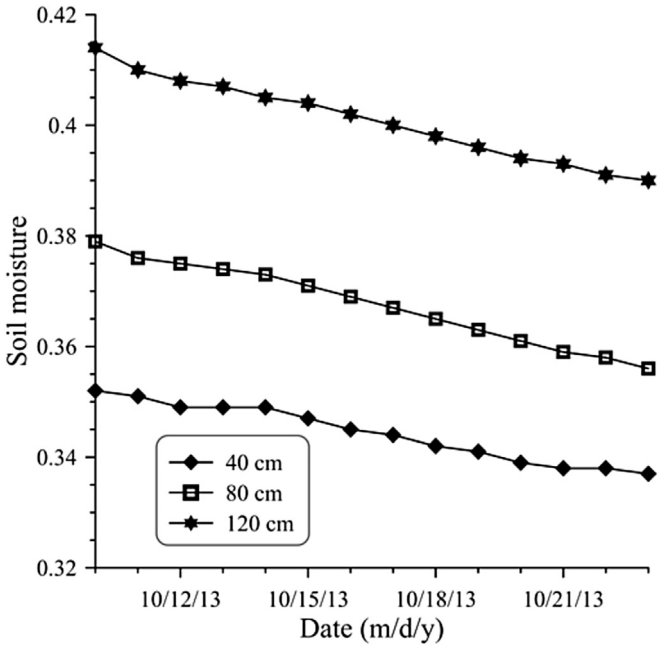

Fig. 6. The variation in the soil moisture dynamics of the active layer during the seasonal freeze process at the AL1 site.

During this stage, the temperature is low in the upper part of the active layer and high in the lower part. The active layer is exothermic. The active layer temperature can be divided into a cooling stage (starting when the whole active layer becomes frozen through to mid- or late January of the following year) and a warming stage (occurring after the cooling stage and until the onset of stable thawing at the ground surface). During the cooling stage, as the active layer temperature decreases, the temperature gradient gradually increases. During the warming stage, as the active layer temperature gradually increases, the temperature gradient gradually decreases (Zhao et al., 2000). The lowest centre of the soil temperature occurred in mid-to late January. The active layer isotherms exhibited a U-shaped distribution, with the bottom of the isotherm's two wings unclosed (Fig. 4). According to Formula (1), the unfrozen water content (UWC) is a power of the absolute value of the negative soil temperature (Xu et al., 2010). Therefore, the lowest centre of the UWC occurred in mid-to late January and the UWC contour lines also exhibited a U-shaped distribution, with the bottom of the isotherm's two wings unclosed. Moreover, the UWC contour lines between 0 °C and −1 °C were intensive (Fig. 4). Unfrozen water migration driven upwards by the temperature gradient is reduced at this stage. Conductive heat transport is the main mode of heat transfer and unfrozen water migration driven by the temperature gradient is also accompanied by heat transport (Zhao et al., 2000).

$$W_u = a|T|^{-b} \quad (1)$$

In Formula (1), W_u is UWC, T is the negative soil temperature, and a and b are empirical constants related to soil factors (both are >0).

5. Discussion

5.1. The influencing factors of the active layer freeze–thaw cycle in the URHHR

The seasonal freeze–thaw cycle of the active layer is influenced by climate conditions, snow cover, vegetation, topography (elevation, aspect and slope), water (swamp water, lakes, rivers and super-permafrost water), lithology and water content (Zhou et al., 2000). Satellite image data analysis showed that the time distribution of the seasonal snow cover was bimodal in the Qilian Mountains and the peaks appeared from October to November and in May of the next year. The frequency and depth of snow were greater from October to November, and the snow rarely appeared in the coldest month of winter (Chen and Chen, 1991). The seasonal snow mainly accumulated in the pass and the shady slope areas of the URHHR. The insulation effect of the snow in winter was dominant in the Dabanshan Pass and the Dadongshushan Pass. The snow provided little cooling effect in the spring, resulting in either no permafrost in these areas or a low boundary of permafrost with an uplifted elevation (Wu et al., 2007). Conversely, the seasonal snow accumulated mainly in the spring and autumn has a cooling effect on the shady slope of the Eboling Mountains Pass, with the lower boundary of continuous alpine permafrost lower by 50–100 m than in the alluvial plain in the west branch. In the study area, occasional snowfall occurred during the spring and autumn, although the snow often melted on the same day. There was significantly more vegetation coverage at the AL1 site than at the others, which in turn had similar vegetation coverage to one another. Vegetation (grass) can reduce the effect of ground surface temperature annual range (GSTAR) as a cooling factor on the QTP, which was a factor causing the reduced ALT observed at the AL1 site. Excluding vegetation, the factors affecting the freeze–thaw cycle of the active layer in the study area are lithology, water content and water.

The seasonal freeze–thaw cycle of the active layer is closely related to the soil's thermo-physical properties, which depend on soil composition, dry density, porosity and water content (Zhou et al., 2000). When dry density and soil water content are equal, the thermal conductivity and thermal diffusivity of the coarse grained soil is greater than that of the fine grained soil. The sand content at depths of 20–100 cm of the active layer at the AL1, AL3, AL4 and AL7 sites increased successively, with values of 28.8, 48.1, 65.4 and 84.2%, respectively (Fig. 7A). Sand content is one of the factors that cause increases in ALT. In addition, with the strong water-holding ability of the organic-rich loam and silty loam, and the high heat consumption of ground ice, the ALT was lowest at the AL1 site.

As the elevation increased from 3700 m a.s.l. to 4132 m a.s.l., the MAGTs of the active layer and the ALTs decreased to 0.18–0.47 °C, −0.27–0.37 °C, −1.28 to −1.20 °C and −1.81 to −1.31 °C, and 3.9 m, 3.6 m, 2.2 m and 1.6 m at the AL7, AL4, AL3 and AL1 sites, respectively (Fig. 7B & Table 1). Considering the difference in the ALTs and the observation depths of the soil temperature at the four sites, the freeze–thaw process at depths of 5–140 cm were compared. As the elevation increased, the onset date of active layer soil freeze occurred earlier, on 24, 20, 16 and 10 October at the AL7, AL4, AL3 and AL1 sites, respectively. Furthermore, the soil freeze rates increased to 2.9 cm d^{-1}, 3.6 cm d^{-1}, 4.4 cm d^{-1} and 20.8 cm d^{-1} at the AL7, AL4, AL3 and AL1 sites, respectively. The onset date of soil thaw and thaw rates, however, did not demonstrate significant trends. The onset dates of soil thaw at the four sites were all in mid- or late April. The thaw rate was lowest at the AL1 site (1.2 cm d^{-1}), with thaw rates of 1.6–2.3 cm d^{-1} at the other sites. It is possible that the seasonal freeze–thaw cycle of the active layer was affected by the elevation, vegetation, lithology, water content and water (swamp water and super-permafrost water). It should be noted that the organic-rich loam and silty loam have a strong water-holding ability, and the soil water content is close to saturation in the summer for a long time. The surface soil water evaporation consumes a lot of heat and a large amount of latent heat is absorbed during the phase transition of the high ground ice content in the

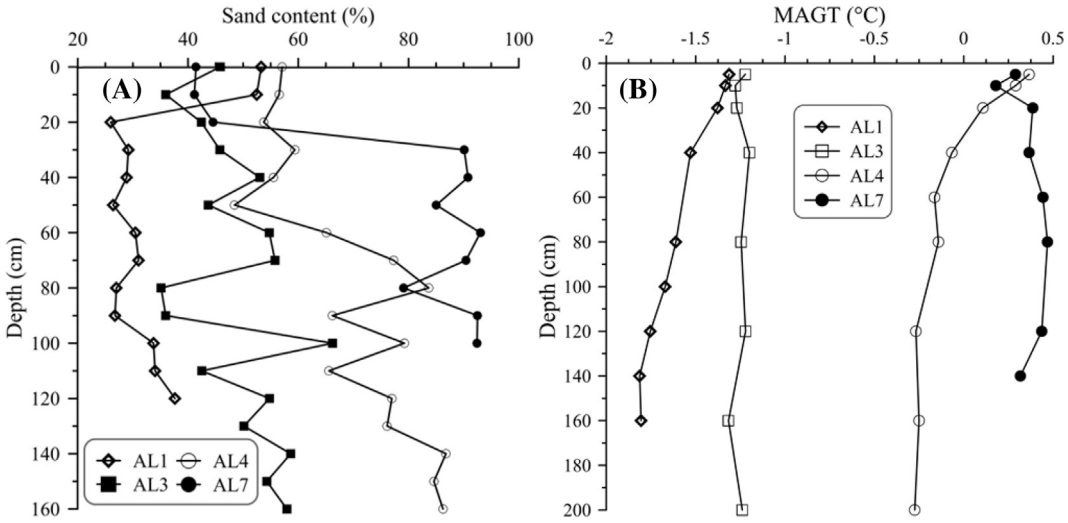

Fig. 7. The (A) sand content distribution and (B) MAGTs of the active layer at four sites.

active layer, especially near the permafrost table, thus causing the lowest soil temperature at the bottom of the active layer and the lowest thaw rate at the AL1 site. In addition, the supply of super-permafrost water delays the freeze–thaw cycle, and the 'zero curtain' formed by the phase change of the ground ice or water remains at a certain depth for an extended period of time.

5.2. The active layer freeze–thaw cycle in the URHHR compared with other places on the QTP

Observations in the Muli Basin in source area of the Datong River in the Qilian Mountains indicated that the snow that was removed can cause the ALT to increase by 0.9–1.0 m and the ground temperature at the bottom of the active layer to increase by 1.1–1.2 °C (Zhou et al., 2000). In the west branch of the Heihe River, the onset dates of soil thaw and freeze at the AL7 site were similar to those of the swamp meadow in the Hulugou Basin. However, the onset dates were delayed compared to those of the alpine cold desert, which occurred in mid-March and mid-September (Yang et al., 2013a). These differences are associated to variations in vegetation, aspect, water (swamp water and super-permafrost water), lithology and water content in the two regions. Compared to the Zuomaoxikong River Basin in the source region of the Yangtze River (Hu et al., 2009b), the onset date of soil thaw and the end date of soil freeze at the four sites in the URHHR occurred significantly earlier, which may have been caused by the MAGTs. With the MAGTs and the onset date of soil freeze close to those of the Maduo Village in the source region of the Yellow River (Luo et al., 2014), the onset dates of soil thaw at the AL3 and AL4 sites were significantly earlier and the ALTs noticeably larger, which is mainly due to the effect of local factors. With the MAGT and the onset date of soil thaw in the hilly regions similar to those of the AL3 site in the south of Wudaoliang, the onset and end dates of soil freeze were significantly earlier and the ALT significantly less (1.5–1.8 m) (Zhao et al., 2000; Wu et al., 2012), which may be the result of the influence of the region's climate conditions, elevation, lithology and water content. Observations along the Qinghai-Tibet Highway, despite similar climate conditions, elevation and onset date of soil thaw, demonstrated ALTs and MAGTs that were rather different (Wu et al., 2012), presumably as a result of differing vegetation coverage, lithology and water content. The findings described above illustrate that the active layer's seasonal freeze–thaw cycle is influenced by very complex factors, such as climate conditions, snow cover, vegetation, topography (elevation, aspect and slope), water, lithology and water content. In the elevation controlled study area, the active layer's seasonal freeze–thaw cycle was also affected by vegetation, topography (elevation, aspect and slope), water (swamp water and super-permafrost water), lithology and water content.

5.3. The moisture migration in the active layer's seasonal freeze and thaw processes

After the active layer's seasonal freeze process from top to bottom, the active layer almost became a closed system. During the active layer's freeze process, the water migrated behind the freeze front. Here, the soil water migrated to the freeze front and led to ice segregation. Migration of unfrozen water and ice segregation also occurred in the frozen soil behind the freeze front (Cheng, 1982). Tests showed that the moisture migration flux in the frozen unsaturated Morin clay in a closed system was proportional to the temperature gradient, was inversely proportional to the square root of the test duration and decreased exponentially with decreasing temperature. The dry density also had an important effect (Xu et al., 2010). Affected by the higher water content near the permafrost table and the freeze rate from bottom to top (less than that from top to bottom), the freeze process from bottom to top was much more conducive to moisture migration and ice segregation, and the amount of moisture migration was greater.

During the thaw process of the active layer from top to bottom, the active layer changed into an open system and the soil moisture migrated to the frozen soil under the thaw front. Ice segregation occurred in the vicinity of the thaw front, the thickness and quantity of which depended on the initial soil water content and dry density. With the new thickened ice and the formation and growth of new ice lenses, a frost heave was produced (Cheng, 1982; Xu et al., 2010). A large number of field observations and laboratory tests all showed that the seasonal thaw process resulted in the redistribution of soil moisture, with soil water content significantly reduced in the thaw layer and significantly increased in the frozen soils (including ice) (Cheng, 1982; Xu et al., 2010). Compared to the onset dates of soil thaw, soil water content at depths of 40 cm, 80 cm and 120 cm at the AL1 site were reduced at the end of the thaw process by 0.086, 0.013 and 0.024, respectively (Fig. 8).

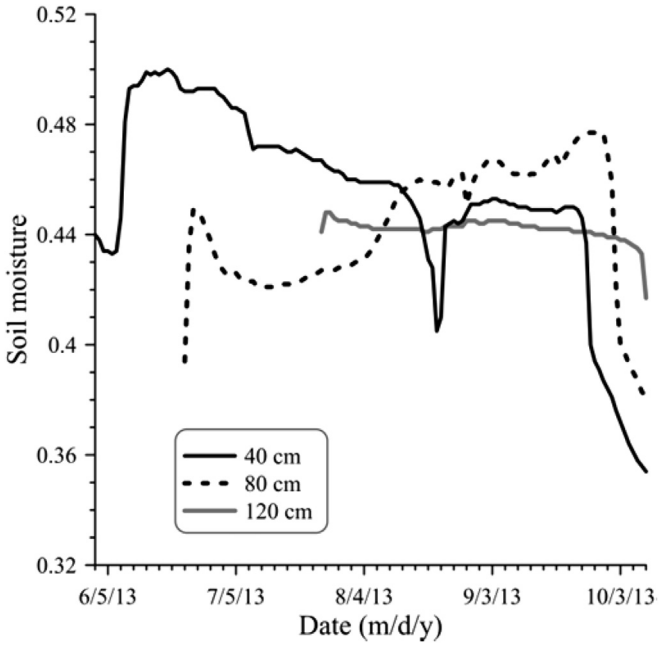

Fig. 8. Variations in the soil moisture dynamics of the active layer in the seasonal thaw process at the AL1 site.

Compared to the bottom to top freeze process, the water supply from outside is abundant during the thaw process. However, the thaw rate is low, especially in the vicinity of the permafrost table. Thus, the amount of moisture migration from top to bottom is greater during the active layer's thaw process, causing the high ice content of the permafrost table (Cheng, 1982).

6. Conclusions and prospects

Using soil temperature, moisture and air temperature data collected from the four active layer observation sites (AL1, AL3, AL4 and AL7) established between Reshuidaban Pass and the low boundary of the alpine permafrost in the alluvial plain in the west branch of the URHHR, from 2013 to 2014, the active layer freeze-–thaw cycle and the soil hydrothermal dynamics were comparatively analysed. The main findings are highlighted below:

(1) Controlled by elevation, the MAGTs of the active layer and the ALTs decreased to 0.18–0.47 °C, −0.27–0.37 °C, −1.28 to −1.20 °C and −1.81 to −1.31 °C, and 3.9 m, 3.6 m, 2.2 m and 1.6 m at the AL7, AL4, AL3 and AL1 sites, respectively, with elevation increasing from 3700 m a.s.l. to 4132 m a.s.l., the onset date of soil freeze occurred earlier on 24, 20, 16 and 10 October at the AL7, AL4, AL3 and AL1 sites, respectively, and the soil freeze rates at depths of 5–140 cm increased to 2.9 cm d^{-1}, 3.6 cm d^{-1}, 4.4 cm d^{-1} and 20.8 cm d^{-1} at the AL7, AL4, AL3 and AL1 sites, respectively. However, affected by local factors, such as vegetation, slope, water (marsh water and super-permafrost water), lithology and water (ice) content, the onset date of soil thaw and the thaw rates did not exhibit significant trends.

(2) Compared to the thaw process, the duration of the active layer freeze process was significantly shortened and its rate was significantly higher. The soil freeze from bottom to top did not occur earlier than that from top to bottom. Furthermore, as elevation increased, the proportion of the bottom-up freeze layer thickness increased from <9% at the AL7 and AL4 sites to 9% at the AL3 site and 37.5% at the AL1 site.

The seasonal freeze–thaw cycle of the active layer and variations in the soil hydrothermal dynamics demonstrate the effects of climate conditions and local factors, which are often intertwined. We need to encourage more comparative studies of different local factors to obtain a quantitative characterisation of their mechanisms and effects on active layers' seasonal freeze–thaw cycles. Such research can provide quantitative data that identify, simulate and predict the hydrological effects of the changes in the permafrost and active layer of the Heihe River Basin. They can also provide a reference for the study of seasonal freeze–thaw cycles and influencing factors in permafrost regions with different climate types, such as other alpine areas in Western China, the northeastern QTP, Northeast China and even in the Arctic or sub-Arctic. In the context of globally widespread permafrost degradation, the identification of the hydrological effects of the changes in the permafrost and active layers has become an important issue for hydrology in cold regions. The ultimate goal is to uncover the trends of groundwater resources in permafrost regions and their responses to global climate change (Cheng and Jin, 2013), and to maintain regional ecological security and sustainable development.

Acknowledgments

This study is supported by the Chinese Academy of Sciences (CAS) Key Research Program (Grant No. KZZD-EW-13), the Natural Science Foundation (NSF) of China (Grant Nos. 91325202, and 41501080), the National Key Scientific Research Program of China (Grant No. 2013CBA01802), the Talent Fund of Cold and Arid Regions Environmental and Engineering Research Institute, CAS (Grant No. 51Y551D71), the State Key Laboratory of Frozen Soil Engineering (Grant No. 52Y452F21), the NSF of China (Grant No. 91025013), and the Strategic Program of the CAS (Grant No. XDA05120302).

References

Arctic Climate Impact Assessment (ACIA), 2005. Impacts of a Warming Climate. Cambridge University Press, Cambridge.

Cao, W.B., Wan, L., Zhou, X., Hu, F.S., Li, Z.M., Liang, S.H., 2003. A study of the geological environment of superapermafrost water in the headwater of the Yellow River. Hydrogeology & Engineering Geology 6, 6–10 (in Chinese with English abstract).

Chang, J., Wang, G.X., Li, C.J., Mao, T.X., 2015a. Seasonal dynamics of supra-permafrost groundwater and its response to the freezing-thawing processes of soil in the permafrost region of Qinghai-Tibet Plateau. Science China Earth Sciences 58, 727–738.

Chang, X.L., Jin, H.J., Zhang, Y.L., He, R.X., Luo, D.L., Wang, Y.P., Lü, L.Z., Zhang, Q.L., 2015b. Thermal impacts of boreal forest vegetation on active layer and permafrost soils in northern Da Xing'anling (Hinggan) Mountains, Northeast China. Arctic, Antarctic, and Alpine Research 47 (2), 47–59.

Chen, Q., Chen, T.Y., 1991. Climatic analysis of seasonal snow in Qilian Mountains. Geographical Research 10 (1), 24–38 (in Chinese with English abstract).

Cheng, G.D., 1982. The forming process of the thick layer underground ice. Science China Chemistry 3, 281–288 (in Chinese with English abstract).

Cheng, G.D., Jin, H.J., 2013. Groundwater in the permafrost regions on the Qinghai-Tibet Plateau and its changes. Hydrogeology & Engineering Geology 4 (1), 1–11 (in Chinese with English abstract).

Hinkel, K.M., Nicholas, J.R.J., 1995. Active layer thaw rate at a boreal forest site in central Alaska, U.S.A. Arctic and Alpine Research 27 (1), 72–80.

Hinzman, L.D., Bettez, N.D., Bolton, W.R., Chapin, F.S., Dyurgerov, M.B., Fastie, C.L., Griffith, B., Hollister, R.D., Hope, A., Huntington, H.P., Jensen, A.M., Jia, G.J., Jorgenson, Y., Kane, D.L., Klein, D.R., Kofinas, G., Lynch, A.H., Lloyd, A.H., McGuire, A.D., Nelson, F.E., Oechel, W.C., Osterkamp, T.E., Racine, C.H., Romanovsky, V.E., Stone, R.S., Stow, D.A., Sturm, M., Tweedie, C.E., Vourlitis, G.L., Walker, M.D., Walker, D.A., Webber, P.J., Welker, F.M., Winker, K.S., Yoshikawa, K., 2005. Evidence and implications of recent climate change in terrestrial regions of the Arctic. Climate Change 72, 251–298.

Hu, H.C., Wang, G.X., Liu, G.S., Li, T.B., Ren, D.X., Wang, Y.B., Cheng, H.Y., Wang, J.F., 2009a. Influences of alpine ecosystem degradation on soil temperature in the freezing-thawing process on Qinghai–Tibet Plateau. Environmental Geology 57, 1391–1397.

Hu, H.C., Wang, G.X., Wang, Y.B., Liu, G.S., Li, T.B., Ren, D.X., 2009b. Response of soil heat-water processes to vegetation cover on the typical permafrost and seasonally frozen soil in the headwaters of the Yangtze and Yellow Rivers.

Chinese Science Bulletin 54 (7), 1225–1233. http://dx.doi.org/10.1007/s11434-008-0532-x.
Li, R., Zhao, L., Ding, Y.J., Wu, T.H., Xiao, Y., Du, E.J., Liu, G.Y., Qiao, Y.P., 2012. Temporal and spatial variations of the active layer along the Qinghai-Tibet Highway in a permafrost region. Chinese Science Bulletin 57 (30), 2864–2871.
Ling, F., Zhang, T., 2006. Sensitivity of ground thermal regime and surface energy fluxes to tundra snow density in northern Alaska. Cold Regions Science and Technology 42 (2), 121–130.
Luo, D.L., Jin, H.J., Lü, L.Z., Wu, Q.B., 2014. Spatiotemporal characteristics of freezing and thawing of the active layer in the source areas of the Yellow River (SAYR). Chinese Science Bulletin 59 (14), 1327–1336 (in Chinese with English abstract).
Mu, C.C., Zhang, T.J., Wu, Q.B., Zhang, X.K., Cao, B., Wang, Q.F., Peng, X.Q., Cheng, G.D., 2014. Stable carbon isotopes as indicators for permafrost carbon vulnerability in upper reach of Heihe River basin, northwestern China. Quaternary International 321, 71–77.
Nicolsky, D.J., Romanovsky, V.E., Alexeev, V.A., Lawrence, D.M., 2007. Improved modeling of permafrost dynamics in a GCM land-surface scheme. Geophysical Research Letters 34, L08501.
Osterkamp, T., Romanovsky, V.E., 1997. Freezing of the active layer on the coastal plain of the Alaskan Arctic. Permafrost Periglacial Process 8, 23–44.
Outcalt, S.I., Hinkel, K.M., 1992. The fractal geometry of thermal and chemical time series from the activer layer, Toolik Lake, Alaska. Physical Geography 13 (4), 273–284.
Outcalt, S.I., Nelson, F.E., Hinkel, K.M., 1990. The zero-curtain effect: heat and mass transfer across an isothermal region in freezing soil. Water Resources Research 26 (7), 1509–1516.
Romanovsky, V.E., Osterkamp, T., 1997. Thawing of the active layer on the coastal plain of the Alaskan Arctic. Permafrost Periglacial Process 8, 1–22.
Serreze, M., Walsh, J., Chapin, F., Osterkamp, T., Dyurgerov, M., Romanovsky, V., Oechel, W.C., Morison, J., Zhang, T., Barry, R.G., 2000. Observational evidence of recent change in the northern high-latitude environment. Climate Change 46, 159–207.
Wang, G.X., Guo, X.Y., Cheng, G.D., 2002. Dynamics variations of landscape pattern and the landscape ecological functions in the source area of the Yellow River. Acta Ecologica Sinica 22 (10), 1587–1598 (in Chinese with English abstract).
Wang, G.X., Hu, H.C., Li, T.B., 2009. The influence of freeze-thaw cycles of active soil layer on surface runoff in a permafrost watershed. Journal of Hydrology 375, 438–449.
Wang, G.X., Li, Y.S., Wang, Y.B., 2008. Synergistic effect of vegetation and air temperature changes on soil water content in alpine frost meadow soil in the permafrost region of Tibet. Hydrology Process 22, 3310–3320.
Wang, G.X., Liu, G.S., Li, C.J., Yang, Y., 2012. The variability of soil thermal and hydrological dynamics with vegetation cover in a permafrost region. Agriculture and Forest Meteorology 162–163, 44–57.
Wang, Q.F., Zhang, T., Wu, J.C., Peng, X.Q., Zhong, X.Y., Mu, C.C., Wang, K., Wu, Q.B., Cheng, G.D., 2013. Investigation on permafrost characteristics over the upper reaches of the Heihe River Basin in Qilian Mountains. Journal of Glaciology and Geocryology 35 (1), 19–29 (in Chinese with English abstract).
Wu, J.C., Sheng, Y., Yu, H., Li, J.P., 2007. Permafrost characteristics in middle east of Qilian Mountains. Journal of Glaciology and Geocryology 29 (3), 418–425 (in Chinese with English abstract).
Wu, Q.B., Hou, Y.D., Yun, H.B., Liu, Y.Z., 2015. Changes in active-layer thickness and near-surface permafrost between 2002 and 2012 in alpine ecosystems, Qinghai–Xizang (Tibet) Plateau, China. Global and Planetary Change 124, 149–155.
Wu, Q., Zhang, T., Liu, Y., 2012. Thermal state of the active layer and permafrost along the Qinghai-Xizang (Tibet) Railway from 2006 to 2010. The Cryosphere 6, 607–612.
Xu, X.Z., Wang, J.C., Zhang, L.X., 2010. Permafrost Physics. Science Press, Beijing, pp. 130–161 (in Chinese).
Yang, Y., Chen, R.S., Ye, B.S., Song, Y.X., Liu, J.F., Han, C.T., Liu, Z.W., 2013a. Heat and water transfer processes on the typical underlying surfaces of frozen soil in cold regions (II). Journal of Glaciology and Geocryology 35 (6), 1555–1563 (in Chinese with English abstract).
Yang, Y.Z., Wu, Q.B., Yun, H.B., 2013b. Stable isotope variations in the ground ice of Beiluhe Basin on the Qinghai-Tibet Plateau. Quaternary International 313–314, 85–91.
Zhang, X., He, J., Zhang, J., Polyakov, I., Gerdes, R., Wu, P., 2013. Enhanced poleward moisture transport and amplified northern high-latitude wetting trend. Nature Climate Change 3, 47–51.
Zhao, L., Cheng, G.D., Li, S.X., Zhao, X.M., Wang, S.L., 2000. Thawing and freezing processes of the active layer in Wudaoliang region of Tibetan Plateau. Chinese Science Bulletin 4 (23), 2181–2187.
Zhao, X.Q., Zhou, H.K., 2005. Eco-environmental degradation, vegetation regeneration and sustainable development in the headwaters of the Three Rivers on the Tibetan Plateau. Bulletin of the Chinese Academy of Sciences 20 (6), 471–476 (in Chinese with English abstract).
Zhou, Y.W., Guo, D.X., Qiu, G.Q., Cheng, G.D., Li, S.D., 2000. Chinese Permafrost. Science Press, Beijing, pp. 81–102 (in Chinese).